

Wave propagation through a random array of pinned dislocations: Velocity change and attenuation in a generalized Granato and Lücke theory

Agnès Maurel,¹ Vincent Pagneux,² Felipe Barra,³ and Fernando Lund^{3,4}

¹*Laboratoire Ondes et Acoustique, UMR CNRS 7587, Ecole Supérieure de Physique et de Chimie Industrielles, 10 rue Vauquelin, 75005 Paris, France*

²*Laboratoire d'Acoustique de l'Université du Maine, UMR CNRS 6613 Avenue Olivier Messiaen, 72085 Le Mans Cedex 9, France*

³*Departamento de Física, Facultad de Ciencias Físicas y Matemáticas, Universidad de Chile, Casilla 487-3, Santiago, Chile*

⁴*Centro para la Investigación Interdisciplinaria Avanzada en Ciencias de los Materiales (CIMAT), Santiago, Chile*

(Received 26 July 2005; revised manuscript received 19 September 2005; published 11 November 2005)

A quantitative theory of the elastic wave damping and velocity change due to interaction with dislocations is presented. It provides a firm theoretical basis and a generalization of the Granato and Lücke model [J. Appl. Phys. **27**, 583 (1956)]. This is done considering the interaction of transverse (T) and longitudinal (L) elastic waves with an ensemble of dislocation segments randomly placed and randomly oriented in an elastic solid. In order to characterize the coherent wave propagation using multiple scattering theory, a perturbation approach is used, which is based on a wave equation that takes into account the dislocation motion when forced by an external stress. In our calculations, the effective velocities of the coherent waves appear at first order in perturbation theory while the attenuations have a part at first order due to the internal viscosity and a part at second order due to the energy that is taken away from the incident direction. This leads to a frequency dependence law for longitudinal and transverse attenuations that is a combination of quadratic and quartic terms instead of the usual quadratic term alone. Comparison with resonant ultrasound spectroscopy (RUS) and electromagnetic acoustic resonance (EMAR) experiments is proposed. The present theory explains the difference experimentally observed between longitudinal and transverse attenuations [Ledbetter, J. Mater. Res. **10**, 1352 (1995)].

DOI: [10.1103/PhysRevB.72.174111](https://doi.org/10.1103/PhysRevB.72.174111)

PACS number(s): 72.10.Fk, 61.72.Lk, 11.80.La, 81.70.Cv

I. INTRODUCTION

Ultrasonic attenuation and velocity change in materials have been shown to be very sensitive to defects, such as dislocations, and their measurement go back at least to the 1950s.¹ In recent years, improvements in experimental and computational techniques have provided a strong motivation to go beyond current theoretical understanding of these phenomena. Indeed, there is now enough accurate data to examine on a quantitative basis the theoretical models. For example, the recent development of the contactless techniques of electromagnetic acoustic resonance (EMAR) and resonant ultrasound spectroscopy (RUS) have greatly increased the accuracy of internal friction measurements in high purity crystals, and it is now possible to differentiate between longitudinal and shear wave effects.^{2–13}

Part of the current theoretical understanding of the elastic wave-dislocation interaction is based on the model of Granato and Lücke^{14–19} developed since the 1950s to the 1980s. That model, that will be discussed in some detail in the body of this paper, considers the response to an external stress wave of an ensemble of damped, stringlike dislocation segments endowed with mass and line tension, subject to viscous loss and pinned between two points. It is a scalar model that captures the essence of the physics of the elastic wave-dislocation interaction. However, it does not consider many complexities of this interaction. For example, it does not differentiate between edge and screw dislocations, nor among the various polarizations available to an elastic wave.

In previous papers,^{20–23} we have studied the interaction of an elastic wave with an ensemble of dislocations in a two

dimensional elastic solid and in the absence of a drag force. These papers presented the theoretical framework in which the elastic wave-dislocation interaction is studied taking into account its full vector nature. The purpose of the present paper is threefold. To generalize the previous work to finite length dislocation segments in three dimensions, to include the effect of viscous drag in the previous framework, and to show that the resulting theory contains the Granato and Lücke theory as a special case. The requisite theory of the interaction of an elastic wave with a single dislocation segment has been developed in Ref. 24 (hereafter Paper I).

The present paper is organized as follows: Section II starts with a form of the theory developed in Paper I that is amenable to a multiple scattering formalism. It is important to remember that the wavelength of the incident wave $2\pi/k$ is assumed to be large compared to the segment length L and to the amplitude of the dislocation motion, introducing a small parameter kL . Then the formalism that is used to study the multiple scattering of an elastic wave by a random distribution of dislocations is introduced. It is based on the derivation of a modified Green function.^{29–31} This is done perturbatively with respect to the small parameter kL at first and second order. The first order results are recovered using Foldy's approach,^{25–28} together with single-scattering results of Paper I. Section III is devoted to the model of Granato and Lücke. It is shown that their approach, based on physical arguments, can be obtained within our framework if it is assumed that dislocation segments are not randomly oriented but have the same orientation, as well as the same Burgers vector and that the incident wave propagates perpendicularly

to the segment direction. A consequence is that a solid filled with such a distribution of dislocations would not be macroscopically isotropic, in contrast with our configuration. Expressions for the attenuation and velocity changes are simply deduced from the effective wave numbers for coherent wave propagation. Section IV discusses the behavior of attenuation and velocity change. It is shown that the attenuation has two terms: a quadratic term due to the internal viscosity and a quartic term due to the multiple scattering process that takes energy away from the incident direction, even in the absence of internal viscosity. The former term appears at first order while the latter term appears at second order in the perturbation approach. However, depending on the value of the drag coefficient, the quadratic and quartic terms may become comparable. Our determination of the attenuation allows us to discriminate between longitudinal and transverse waves and comparison with EMAR measurements is performed. In Sec. V we present concluding remarks. Some useful but well known relations and technical calculations are collected in the appendices.

II. MULTIPLE SCATTERING BY A RANDOM DISTRIBUTION OF PINNED DISLOCATION SEGMENTS

We shall use the formalism and notation introduced in Paper I. When many dislocation segments are present, it is usual to define the total length of movable dislocation per unit volume Λ instead of the density of dislocation segments n ,

$$\Lambda \equiv Ln. \quad (2.1)$$

For a fixed Λ , the length L of dislocation segments between two pinners can change because of a change in the density of impurity atoms. This is the picture of the change in L during holding stress tests or compression tests, where Λ is assumed to remain constant while the point defects migrate to the dislocation lines and pin them into smaller segments, decreasing L .

Our results are valid in a low frequency approximation meaning that $kL \ll 1$ or $\omega/\omega_1 \ll 1$, where $\omega_1 = c_T \pi/L$ (as it will be seen below in this section). With $c_T \approx 3 \times 10^3$ m/s and typical micrometer dislocation length L , we get ω_1 around few GHz. Usual experiments occur in the kHz to MHz frequency range and only some very recent experiments reach the GHz range.^{32–34} We can thus conclude that the low frequency regime approximation is largely satisfied in the kHz and MHz frequency ranges, while the GHz frequency regime falls in the limit of validity of our approximation, so that our derivation should be revisited in that case.

The basic mechanism for the wave scattering, whose detailed derivation can be found in Sec. II of Paper I, is as follows: The incident wave hits the dislocation, causing it to oscillate in response.^{35–39} This motion follows

$$\dot{X}(s, \omega) = -\frac{4}{\pi} \frac{\mu b}{m} \tilde{S}(s, \omega) \mathbf{M}_{lk} \partial_l v_k(\mathbf{X}_0, \omega), \quad (2.2)$$

as in Eq. (2.7) in Paper I. The ensuing oscillatory motion generates outgoing (from the dislocation position) elastic waves, whose velocity field is given by

$$v_m^s(\mathbf{x}, t) = \epsilon_{jnh} c_{ijkl} \int_{\mathcal{L}} \int_{\mathcal{L}} dt' ds b_i \dot{X}_n(s, t') \tau_h \times \frac{\partial}{\partial x_l} G_{km}^0(\mathbf{x} - \mathbf{X}_0, t - t'), \quad (2.3)$$

as in Eq. (2.11) in Paper I. The scattered field given by Eq. (2.3) can be viewed equivalently as the solution of the following modified wave equation, that accounts for the discontinuity relation through a source term:

$$\rho \frac{\partial^2}{\partial t^2} v_i(\mathbf{x}, t) - c_{ijkl} \frac{\partial^2}{\partial x_j \partial x_l} v_k(\mathbf{x}, t) = s_i(\mathbf{x}, t), \quad (2.4)$$

with

$$s_i(\mathbf{x}, t) = c_{ijkl} \epsilon_{mnk} \int_{\mathcal{L}} ds \dot{X}_m(s, t) \tau_n b_l \frac{\partial}{\partial x_j} \delta(\mathbf{x} - \mathbf{X}_0). \quad (2.5)$$

To see that Eq. (2.4) is the proper equation to study, it is sufficient to remark that its solution is the convolution of the Green function of free space with the source term

$$v_m^s(\mathbf{x}, t) = \int dt' d\mathbf{x}' G_{km}^0(\mathbf{x} - \mathbf{x}', t - t') s_k(\mathbf{x}', t'). \quad (2.6)$$

Writing the integral representation in Eq. (2.3) as

$$v_m^s(\mathbf{x}, t) = \int dt' d\mathbf{x}' \epsilon_{jnh} c_{ijkl} \int_{\mathcal{L}} ds b_i \dot{X}_n(s, t') \tau_h \times \frac{\partial}{\partial x_l} G_{km}^0(\mathbf{x} - \mathbf{X}_0, t - t') \delta(\mathbf{x}' - \mathbf{X}_0) = \int dt' d\mathbf{x}' G_{km}^0(\mathbf{x} - \mathbf{x}', t - t') \epsilon_{jnh} c_{ijkl} \times \int_{\mathcal{L}} ds b_i \dot{X}_n(s, t') \tau_h \frac{\partial}{\partial x_l} \delta(\mathbf{x}' - \mathbf{X}_0). \quad (2.7)$$

$s_k(\mathbf{x}, t)$ in Eq. (2.5) is simply obtained identifying Eq. (2.7) with Eq. (2.6).

The next step consists in writing the source term of Eq. (2.5) using Eq. (2.2). We get

$$s_i(\mathbf{x}, \omega) = \frac{8}{\pi^2} \frac{\mu b}{m} \frac{S(\omega)}{\omega^2} L c_{ijkl} n_k b_l \frac{\partial}{\partial x_j} \delta(\mathbf{x} - \mathbf{X}_0) \mathbf{M}_{lk} \frac{\partial}{\partial x_l} v_k(\mathbf{X}_0, \omega), \quad (2.8)$$

where we have used $\epsilon_{kmn} \dot{X}_m \tau_n = -\dot{X}_k$ and with

$$S(\omega) \equiv \frac{\pi \omega^2}{2L} \int_{-L/2}^{L/2} ds \tilde{S}(s, \omega) \approx \frac{\omega^2}{\omega^2 - \omega_1^2 + i\omega B/m}. \quad (2.9)$$

We now use $c_{ijkl} n_k b_l = \mu b \mathbf{M}_{ij}$ to get

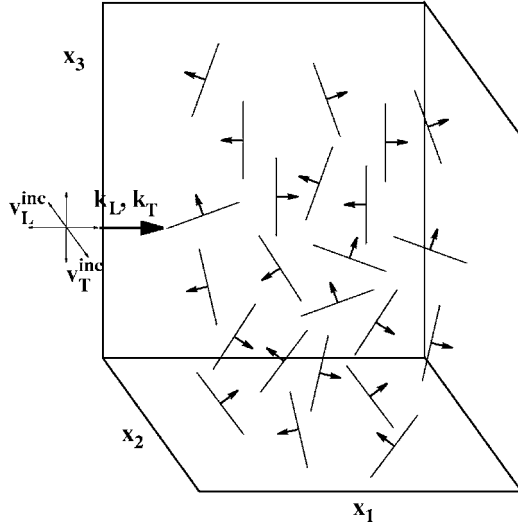


FIG. 1. Configuration for the study of multiple scattering, the incident wave has transverse (T) and longitudinal (L) polarizations and propagates through an ensemble of randomly distributed and oriented dislocation segments with pinned ends. Each segment is of variable length L and its Burgers vector is of variable modulus.

$$s_i(\mathbf{x}, \omega) = \frac{8}{\pi^2} \frac{(\mu b)^2 S(\omega)}{m \omega^2} L M_{ij} \frac{\partial}{\partial x_j} \delta(\mathbf{x} - \mathbf{X}_0) M_{lk} \frac{\partial}{\partial x_l} v_k(\mathbf{X}_0, \omega), \quad (2.10)$$

and use it to define the “potential” V_{ik} through $s_i = V_{ik} v_k$ in Eq. (2.4),

$$V_{ik} = \frac{8}{\pi^2} \frac{(\mu b)^2 S(\omega)}{m \omega^2} L M_{ij} \frac{\partial}{\partial x_j} \delta(\mathbf{x} - \mathbf{X}_0) M_{lk} \frac{\partial}{\partial x_l |_{\mathbf{x}=\mathbf{X}_0}}. \quad (2.11)$$

The source term in Eq. (2.10) and potential in Eq. (2.11) describe the interaction of a single moving dislocation line with the elastic wave. For a distribution of N dislocation lines, the resulting source term and potential are simply obtained by superposition. In this way, the formalism developed in Paper I is ready for generalization to multiple scattering.

The configuration of interest for multiple scattering is shown in Fig. 1. Multiple scattering is generally quite involved. However, there may exist a coherent wave propagating with an effective wave velocity, its amplitude being attenuated because of the energy scattered away from the direction of propagation. We present in this section the derivation of the coherent wave using the formalism of the modified Green function.^{29–31}

In this section, $\mathbf{P}_{\hat{\mathbf{k}}} \equiv \hat{\mathbf{k}} \hat{\mathbf{k}}$ denotes the projector along the $\hat{\mathbf{k}}$ direction ($\hat{\mathbf{k}} \equiv \mathbf{k}/k$ denotes the unitary vector along \mathbf{k}).

A. Parameters of the average

In the theory of coherent propagation, the coherent wave propagates in an effective medium that corresponds to the average over all realizations of the disordered medium. One realization corresponds to $N(\gg 1)$ dislocation segments, each

segment being characterized by, as described in Paper I, (i) its location \mathbf{X}_0 and its orientation given by the Euler angles $\Omega = (\theta, \varphi, \xi)$ through $(\hat{\mathbf{b}}, \boldsymbol{\tau}) = \mathbf{R}(\mathbf{e}_1, \mathbf{e}_3)(\hat{\mathbf{b}} \equiv \mathbf{b}/b)$, where \mathbf{R} is the rotation of Euler angles defined in Eq. (A1), (ii) the value of the Burgers vector modulus b and the length L of the segment. The probability function for a quantity x is denoted $p(x)$. Finally, assuming that the dislocation locations are uncorrelated, that the dislocations are uniformly distributed in a volume \mathcal{V} [$p(\mathbf{X}_0) = 1/\mathcal{V}$], and uniformly oriented [$p(\Omega) = 1/8\pi^2$], averages are performed using the integrand

$$d\mathbf{C} = \frac{d\mathbf{X}_0 d\Omega}{\mathcal{V} 8\pi^2} p(b) db p(L) dL. \quad (2.12)$$

The assumption that $(\hat{\mathbf{b}}, \boldsymbol{\tau})$ can take any orientation could be simply modified to account for a particular anisotropy (see for instance Sec. III). In contrast, adding a correlation between scatterers leads to significant complications.

In our calculations, the averages of the modulus b of the Burgers vector can be performed with any probability function, without restriction. However, for the sake of simplicity, we continue to use the notation b^2 for $\int db b^2 p(b)$, so in the following, b has to be understood as an average value. In contrast, averaging over L is less straightforward and we shall consider L constant in the following.

B. Modified Green function approach

Following the usual multiple scattering notation, we denote by G^0 the Green tensor for the wave equation in free space and by G the Green tensor for the wave equation modified in the presence of a given realization of random distribution of dislocation segments,

$$\begin{aligned} \rho \omega^2 G_{im}^0(\mathbf{x}, \omega) + c_{ijkl} \frac{\partial^2}{\partial x_j \partial x_l} G_{km}^0(\mathbf{x}, \omega) &= -\delta_{im} \delta(\mathbf{x}), \\ \rho \omega^2 G_{im}(\mathbf{x}, \omega) + c_{ijkl} \frac{\partial^2}{\partial x_j \partial x_l} G_{km}(\mathbf{x}, \omega) &= -\sum_{\text{disloc. lines}} V_{ik} G_{km}(\mathbf{x}, \omega) - \delta_{im} \delta(\mathbf{x}), \end{aligned} \quad (2.13)$$

where V is the “potential” [Eq. (2.11)] that describes the effect of a single dislocation segment. Properties of G^0 relevant to our treatment are collected in Appendix B.

In the multiple scattering formalism, the effective wave numbers K_a ($a=L, T$) characterize the coherent wave propagation in an effective medium, defined as the average over all random distributions of dislocation segments.^{20,29–31} The wave numbers are the poles of the modified, averaged, Green function $\langle G \rangle$, related to the Green tensor in free space through the Dyson equation

$$\langle G \rangle = [(G^0)^{-1} - \Sigma]^{-1}, \quad (2.14)$$

where Σ is the mass operator, whose relation to V is, in general, quite involved. For weak scattering, Σ can be developed in perturbation theory for small V , to first and second order,

$$\Sigma = \Sigma^{(1)} + \Sigma^{(2)}$$

with

$$\Sigma_{ik}^{(1)}(\mathbf{k}) = n \int d\mathbf{x} d\mathbf{C} e^{-i\mathbf{k}\mathbf{x}} V_{ik}(\mathbf{x}) e^{i\mathbf{k}\mathbf{x}},$$

$$\Sigma_{ij}^{(2)}(\mathbf{k}) = n \int d\mathbf{x} d\mathbf{x}' d\mathbf{C} e^{-i\mathbf{k}\mathbf{x}} V_{in}(\mathbf{x}) G_{nl}^0(\mathbf{x} - \mathbf{x}') V_{lj}(\mathbf{x}') e^{i\mathbf{k}\mathbf{x}'}, \quad (2.15)$$

where n is the number of dislocation segments per unit volume and the integral over \mathbf{C} corresponds to the average over all realizations of random distributions, as in Eq. (2.12). The calculations are detailed in Appendix C. The interest in the calculation at second order is to determine the attenuation due to the multiple scattering process that occurs even in the absence of internal viscosity. Thus, only the imaginary part of $\Sigma^{(2)}$ is used. We get

$$\Sigma^{(1)}(\mathbf{k}) = -\rho c_T^2 k^2 s_1 [\mathbf{P}_{\hat{\mathbf{k}}} + 3\mathbf{I}], \quad \text{with } s_1 = \frac{8}{15\pi^2} \frac{\rho b^2 S(\omega)}{m \omega^2} n L c_T^2,$$

$$\text{Im}[\Sigma^{(2)}(\mathbf{k})] = -\rho c_T^2 k^2 s_2 [\mathbf{P}_{\hat{\mathbf{k}}} + 3\mathbf{I}], \quad \text{with}$$

$$s_2 = -\frac{32}{225\pi^5} \frac{3\gamma^5 + 2}{\gamma^5} \left(\frac{\rho b^2}{m}\right)^2 \frac{\text{Re}[S^2(\omega)]}{\omega} n L^2 c_T.$$

Equation (2.14) being algebraic in Fourier space, it allows for the derivation of the effective wave numbers as the poles of $\langle G \rangle(\mathbf{k})$. With $G^{0-1}(\mathbf{k}) = \rho [c_T^2(k^2 - k_T^2)(1 - \mathbf{P}_{\hat{\mathbf{k}}}) + c_L^2(k^2 - k_L^2)\mathbf{P}_{\hat{\mathbf{k}}}]$, we get

$$\langle G \rangle^{-1} = \rho c_T^2 \{ [1 + 3(s_1 + i s_2)] k^2 - k_T^2 \} (1 - \mathbf{P}_{\hat{\mathbf{k}}}) + \rho c_L^2 \{ [1 + 4\gamma^{-2}(s_1 + i s_2)] k^2 - k_L^2 \} \mathbf{P}_{\hat{\mathbf{k}}}, \quad (2.16)$$

from which it is easily found that the effective wave numbers K_a ($a=L, T$) are

$$K_L \simeq k_L \left[1 - \frac{16}{15\pi^2} \frac{1}{\gamma^4} \frac{\rho b^2 S(\omega)}{m \omega^2} n L c_L^2 + i \frac{64}{225\pi^5} \frac{3\gamma^5 + 2}{\gamma^8} \left(\frac{\rho b^2}{m}\right)^2 \frac{\text{Re}[S^2(\omega)]}{\omega} n L^2 c_L \right],$$

$$K_T \simeq k_T \left[1 - \frac{4}{5\pi^2} \frac{\rho b^2 S(\omega)}{m \omega^2} n L c_T^2 + i \frac{16}{75\pi^5} \frac{3\gamma^5 + 2}{\gamma^5} \left(\frac{\rho b^2}{m}\right)^2 \frac{\text{Re}[S^2(\omega)]}{\omega} n L^2 c_T \right]. \quad (2.17)$$

It is shown in Appendix D that the first order result is easily recovered using Foldy's approach,²⁵⁻²⁸ where multiple scattering is inferred from the response of a single scatterer.

Let us first comment on the results obtained at second order with the modified Green function. With typically $K \sim k[1 + nL^3(1 + (kL)^3)]$ in Eqs. (2.17), weak scattering means here

(1) small $\epsilon' = nL^3$. This assumption, with $nL^3 = \Lambda L^2$, is

reasonably verified with typical micrometer L , and Λ ranging from 10^8 to 10^{10} m^{-2} .

(2) small $\epsilon = kL$ value. As previously mentioned, this low frequency regime is verified in most experiments.

Finally, the phase velocities $v_a = \omega / \text{Re}(K_a)$, $a=L, T$ are obtained from Eqs. (2.17). At first order, they are

$$v_L \simeq c_L \left(1 + \frac{16}{15\pi^2} \frac{1}{\gamma^4} \frac{\rho b^2}{m} c_L^2 \Lambda \frac{\omega^2 - \omega_1^2}{(\omega^2 - \omega_1^2)^2 + \omega^2 B^2 / m^2} \right),$$

$$v_T \simeq c_T \left(1 + \frac{4}{5\pi^2} \frac{\rho b^2}{m} c_T^2 \Lambda \frac{\omega^2 - \omega_1^2}{(\omega^2 - \omega_1^2)^2 + \omega^2 B^2 / m^2} \right). \quad (2.18)$$

The attenuation $\alpha_a \equiv \text{Im}(K_a)$ has two origins. Because of the internal viscosity, the first order gives a contribution in B to the attenuation. The contribution at second order is due to the multiple scattering process that takes energy away from the incident direction. This latter attenuation exists even for $B=0$. We get

$$\alpha_L = \frac{16}{15\pi^2} \frac{1}{\gamma^4} \frac{\rho b^2}{m} \Lambda L \left(\frac{c_L B}{L m} \frac{\omega^2}{(\omega^2 - \omega_1^2)^2 + \omega^2 B^2 / m^2} + \frac{4(3\gamma^5 + 2)}{15\pi^3 \gamma^4} \frac{\rho b^2}{m} \frac{\omega^4 [(\omega^2 - \omega_1^2)^2 - \omega^2 B^2 / m^2]}{[(\omega^2 - \omega_1^2)^2 + \omega^2 B^2 / m^2]^2} \right),$$

$$\alpha_T = \frac{4}{5\pi^2} \frac{\rho b^2}{m} \Lambda L \left(\frac{c_T B}{L m} \frac{\omega^2}{(\omega^2 - \omega_1^2)^2 + \omega^2 B^2 / m^2} + \frac{4(3\gamma^5 + 2)}{15\pi^3 \gamma^5} \frac{\rho b^2}{m} \frac{\omega^4 [(\omega^2 - \omega_1^2)^2 - \omega^2 B^2 / m^2]}{[(\omega^2 - \omega_1^2)^2 + \omega^2 B^2 / m^2]^2} \right). \quad (2.19)$$

Simplified expressions are presented in Sec. IV.

III. DISCUSSION OF THE GRANATO AND LÜCKE MODEL

The Granato and Lücker model (hereafter referred to as the GL model) has been widely used to interpret experimental results. It is a scalar model whose starting point is the following set of equations:

$$\rho \frac{\partial^2}{\partial t^2} \sigma(\mathbf{x}, t) - \mu \frac{\partial^2}{\partial x_2^2} \sigma(\mathbf{x}, t) = -\mu \rho b \frac{\Lambda}{L} \int ds \ddot{\xi}(\mathbf{x}, s, t),$$

$$m \ddot{\xi} + B \dot{\xi} - \Gamma \xi'' = \mu \sigma, \quad (3.1)$$

where Λ is defined in Eq. (2.1) as the total length of movable dislocation per unit volume. The system is then solved looking for a solution of the form

$$\sigma(x_2, t) = \sigma_0 e^{-\alpha_{GL} x_2} e^{i\omega(t - x_2/v_{GL})}, \quad (3.2)$$

assuming ξ independent of x_3 . While this system of equations is eminently reasonable on physical grounds, to the best of our knowledge it has not been derived from the vector equations of elasticity in conjunction with the vector equations of dislocations dynamics.

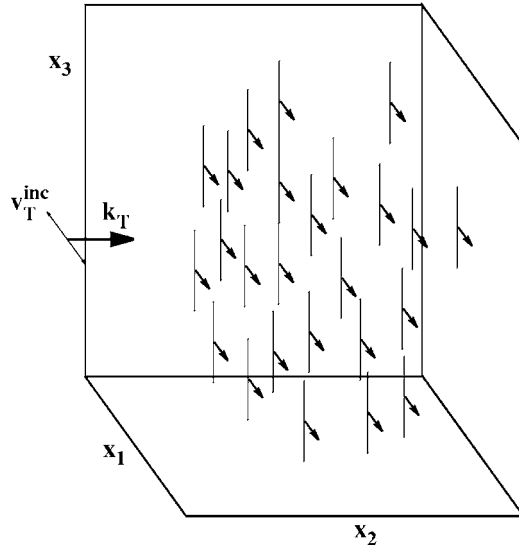


FIG. 2. Configuration of the GL model, the incident wave has only transverse polarization and propagates through an ensemble of randomly distributed dislocation segments having the same orientation along \mathbf{e}_3 and the same gliding direction along \mathbf{e}_1 , and they are pinned at both ends. The dislocation segments can be of variable Burgers vector modulus b . This picture must be contrasted with the general case of our present study in Fig. 1.

The solution for the stress σ proposed by GL shows that the system of equations is considered for averaged quantities. Indeed, the interaction of an incident wave with a single dislocation segment leads to a scattering process unable to produce a plane wave (see Refs. 23,24). In contrast, the solution (3.2) has the typical form of the solution for effective propagation.

It is shown in this section that the GL model is indeed recovered within the framework of our multiple scattering formalism when the dislocation segments are randomly placed but not randomly oriented. Rather, when they all point along the same direction, as depicted in Fig. 2. Note, for contrast, the more general configuration of the present study (Fig. 1).

A. The configuration of the GL model

The GL model focuses on the behavior of an incident wave propagating along the \mathbf{e}_2 direction, that is, perpendicular to both the dislocation and the Burgers vector. This has an important consequence since, in that case, only the shear wave with polarization along the Burgers vector interacts with the dislocation segment. This can be seen in the scattering amplitudes provided in Eqs. (3.5) of Paper I, with $\theta_0 = \pi/2$, $\varphi_0 = 0$, we get $f_L = 0$ meaning that the incident longitudinal wave does not give rise to a scattered wave along that direction. Also, with $f_T = -\cos \xi_0$ (here ξ_0 gives the direction of the transverse polarization with the \mathbf{e}_1 axis of the Burgers vector), only the component parallel to the Burgers vector interacts with the dislocation segment ($\xi_0 = 0$). This is why the GL model is a scalar model.

The system of equations (3.1) is composed of a modified wave equation for the stress σ coupled with an equation of

motion for the displacement ξ . The equation of motion is the same as our Eq. (2.1) in Paper I. Here, the gliding motion occurs along the \mathbf{e}_1 direction, so that the Peach-Koehler force along that direction reduces to $F_1 = b\sigma_{12}$. In the following, we adopt the GL notation with $\sigma \equiv \sigma_{12}$. The next step is to show that Eq. (3.1), a modified wave equation for σ , is similar to our Eq. (2.4).

To recover this modified wave equation, we use the same procedure used to obtain our Eq. (2.4). We start from the integral representation for the stress tensor, whose detailed derivation can be found in Appendix E,

$$\sigma(\mathbf{x}, t) = -\mu\rho b \int \int_{\mathcal{L}} dt' ds \dot{X}(s, t') \frac{\partial}{\partial t} G^0[\mathbf{x} - \mathbf{X}_0, t - t'], \quad (3.3)$$

where $G^0 \equiv G_{11}^0$ is the Green function in free space for scalar shear waves. Identifying terms in the integral representation for a convolution, $\int dt' d\mathbf{x}' G^0(\mathbf{x} - \mathbf{x}', t - t') s(\mathbf{x}', t')$, we easily get the source term in the modified wave equation for σ ,

$$\rho \frac{\partial^2}{\partial t^2} \sigma(\mathbf{x}, t) - \mu \frac{\partial^2}{\partial x_2^2} \sigma(\mathbf{x}, t) = s(\mathbf{x}, t)$$

with

$$s(\mathbf{x}, t) = -\mu\rho b \int_{\mathcal{L}} ds \ddot{X}(s, t) \delta(\mathbf{x} - \mathbf{X}_0), \quad (3.4)$$

where \mathbf{X} has been taken equal to \mathbf{X}_0 in the limit $kL \ll 1$. As stated, Eq. (3.4) clearly differs from the first equation in (3.1) because our Eq. (3.4) concerns a single scatterer. Thus, one needs to average this equation, which is done as follows: Consider an ensemble of N dislocation segments as shown in Fig. 2, all parallel to \mathbf{e}_3 and having a Burgers vector b along \mathbf{e}_1 . The displacements ξ for each segment depend on the position of the center \mathbf{X}_0^i , $i = 1, \dots, N$, so that we denote in the following $\xi = \xi(\mathbf{X}_0^i, s, t)$. The source term for this ensemble of dislocation segments is simply obtained by superposition and the stress satisfies the new modified wave equation,

$$\rho \frac{\partial^2}{\partial t^2} \sigma(\mathbf{x}, t) - \mu \frac{\partial^2}{\partial x_2^2} \sigma(\mathbf{x}, t) = - \sum_{i=1}^N \mu\rho b \int_{\mathcal{L}} ds \ddot{X}(X_0^i, s, t) \times \delta(\mathbf{x} - \mathbf{X}_0^i), \quad (3.5)$$

where we keep the same notation σ for simplicity. Consider now all possible realizations of the positions $(\mathbf{X}_0^i)_{i=1, \dots, N}$ in a volume \mathcal{V} . Assuming that there is no correlation between these positions, we can perform the average as

$$\rho \frac{\partial^2}{\partial t^2} \sigma(\mathbf{x}, t) - \mu \frac{\partial^2}{\partial x_2^2} \sigma(\mathbf{x}, t) = -\mu\rho b \int \frac{d\mathbf{X}_0^1}{\mathcal{V}} \dots \frac{d\mathbf{X}_0^N}{\mathcal{V}} \times \sum_{i=1}^N \int_{\mathcal{L}} ds \ddot{X}(\mathbf{X}_0^i, s, t) \delta(\mathbf{x} - \mathbf{X}_0^i). \quad (3.6)$$

The stress σ on the left-hand-side term should be replaced by the mean stress resulting from the average process but

again, for simplicity, we keep the same notation. It is now sufficient to note that the right-hand side term is formed of N identical terms

$$\begin{aligned} & -\mu\rho b \int \frac{d\mathbf{X}_0}{\mathcal{V}} \int_{\mathcal{L}} ds \ddot{X}(\mathbf{X}_0, s, t) \delta(\mathbf{x} - \mathbf{X}_0) \\ & = -\mu\rho b \frac{1}{\mathcal{V}} \int_{\mathcal{L}} ds \ddot{X}(\mathbf{x}, s, t). \end{aligned} \quad (3.7)$$

Finally, the averaged modified wave equation is

$$\rho \frac{\partial^2}{\partial t^2} \sigma(\mathbf{x}, t) - \mu \frac{\partial^2}{\partial x_2^2} \sigma(\mathbf{x}, t) = -\mu\rho b n \int_{\mathcal{L}} ds \ddot{X}(\mathbf{x}, s, t), \quad (3.8)$$

where $n \equiv N/\mathcal{V}$ is the density of dislocation segments. With $nL = \Lambda$ and $\ddot{X} = \ddot{\xi}$, the above Eq. (3.8) is the same as the first Granato and Lücke Eq. (3.1).

B. Comparison of the results on attenuation and velocity change

The change in velocity and the attenuation are found in the GL model by solving the system of Eqs. (3.1) and (3.2) to get

$$\begin{aligned} v_{\text{GL}} &= c_T \left(1 + \frac{4}{\pi^2} \frac{\rho b^2}{m} n L c_T^2 \frac{\omega^2 - \omega_1^2}{(\omega^2 - \omega_1^2)^2 + \omega^2 B^2 / m^2} \right), \\ \alpha_{\text{GL}} &= \frac{4}{\pi^2} \frac{\rho b^2}{m} n L c_T \frac{\omega^2 B / m}{(\omega^2 - \omega_1^2)^2 + \omega^2 B^2 / m^2}. \end{aligned} \quad (3.9)$$

These expressions differ from our results for transverse wave in Eqs. (2.18) and (2.19) at first order by a numerical constant 1/5.

It is easily checked that (3.9) can be recovered within our formalism: It is sufficient, for the calculation of the mass operator, to note that the operator $\mathbf{M} \hat{\mathbf{k}}^i \hat{\mathbf{k}}^m$ in Eq. (C2), that was averaged over the Euler angles to account for all possible orientations of the segments and of the Burgers vectors, must be calculated here with a fixed $\mathbf{M} = \mathbf{e}_1^t \mathbf{e}_2 + \mathbf{e}_2^t \mathbf{e}_1$, without averaging. We get, from Eqs. (B3) and (C2) that the effective wave numbers are given by the poles of $\langle G \rangle^{-1}(\mathbf{k})$ with

$$\langle G \rangle^{-1}(\mathbf{k}) = G^{0-1}(\mathbf{k}) - \Sigma(\mathbf{k}), \quad (3.10)$$

with

$$\begin{aligned} \Sigma(\mathbf{k}) &= -\rho c_T^2 s_1 \begin{pmatrix} k_2^2 & k_1 k_2 & 0 \\ k_1 k_2 & k_1^2 & 0 \\ 0 & 0 & 0 \end{pmatrix}, \quad \text{and} \\ s_1 &= \frac{8}{\pi^2} \frac{\rho b^2}{m} \frac{S(\omega)}{\omega^2} n L c_T^2. \end{aligned} \quad (3.11)$$

Using $\hat{\mathbf{k}} = [\cos \varphi \cos \theta; \cos \varphi \sin \theta; \sin \varphi]$, it is straightforward to find the determinant of $\langle G \rangle^{-1}$,

$$\begin{aligned} \Delta_{\langle G \rangle} &= \rho c_T^2 (k^2 - k_T^2) \{ (k^2 - k_T^2) (\gamma^2 k^2 - k_T^2) + s_1 k^2 \cos^2 \varphi [k^2 - k_T^2 \\ &+ (\gamma^2 - 1) k^2 f(\theta, \varphi)] \}, \end{aligned} \quad (3.12)$$

with $f(\theta, \varphi) = 1 - \cos^2 \varphi \sin^2 2\theta$. The modified wave numbers being close to the wave numbers k_L , k_T , we can calculate their values at leading order in s_1 ,

$$\begin{aligned} K_T &= k_T \left(1 - \frac{s_1}{2} \cos^2 \varphi f(\theta, \varphi) \right), \\ K_L &= k_L \left(1 - \frac{s_1}{2\gamma^2} \cos^2 \varphi [1 - f(\theta, \varphi)] \right). \end{aligned} \quad (3.13)$$

The modified wave numbers K_a , $a=L, T$ are illustrated in Fig. 3, the deviation from a spherical shape illustrates the anisotropy of this medium. Another configuration, where the lines are parallel with a randomly oriented Burgers vector in the plane perpendicular to $\boldsymbol{\tau}$ is treated in Appendix F. In the case considered by GL, the incident wave is along \mathbf{e}_2 ($\varphi=0$, $\theta=\pi/2$, so that $f=1$), the longitudinal wave does not interact with the dislocations, the wave numbers of the acoustic L wave and of the shear T wave whose polarization is along the segment direction, are not modified. In contrast, the shear T wave whose polarization is along the Burgers vector is modified and its effective wave number is

$$K_T \simeq k_T \left(1 - \frac{4}{\pi^2} \frac{\rho b^2}{m} S(\omega) L \frac{n}{k_T^2} \right), \quad (3.14)$$

in agreement with the expressions of the velocity change and of the attenuation in Eqs. (3.9).

IV. VELOCITY CHANGES AND ATTENUATION: DISCUSSION ON THE QUALITY Q^{-1} -FACTOR IN EMAR AND RUS EXPERIMENTS

A. Velocity changes and attenuations

We use in the following

$$\omega_m \equiv \frac{m\omega_1^2}{B} = \pi^2 \frac{\Gamma}{BL^2}, \quad (4.1)$$

[note that $\omega_m = (B_c/2B)\omega_1$, with B_c defined in Eq. (2.10) in Paper I]. In the limit $\omega \ll \omega_1$, the phase velocities and velocity changes defined in Eqs. (2.18) and (2.19) can be written in the simplified form

$$\begin{aligned} v_L &\simeq c_L \left(1 - \frac{16}{15\pi^4} \frac{1}{\gamma^2} \frac{\mu b^2}{\Gamma} \Lambda L^2 \frac{1}{1 + (\omega/\omega_m)^2} \right), \\ v_T &\simeq c_T \left(1 - \frac{4}{5\pi^4} \frac{\mu b^2}{\Gamma} \Lambda L^2 \frac{1}{1 + (\omega/\omega_m)^2} \right), \\ \alpha_L &= \frac{16}{15\pi^6} \frac{1}{\gamma^2} \frac{\mu b^2 \Lambda L^4 B \omega^2}{c_L \Gamma^2} \left(\frac{1}{1 + (\omega/\omega_m)^2} \right. \\ &\quad \left. + \frac{4(3\gamma^5 + 2)}{15\pi^3 \gamma^4} \frac{\rho b^2 L}{c_L B} \omega^2 \frac{1 - (\omega/\omega_m)^2}{[1 + (\omega/\omega_m)^2]^2} \right), \end{aligned} \quad (4.2)$$

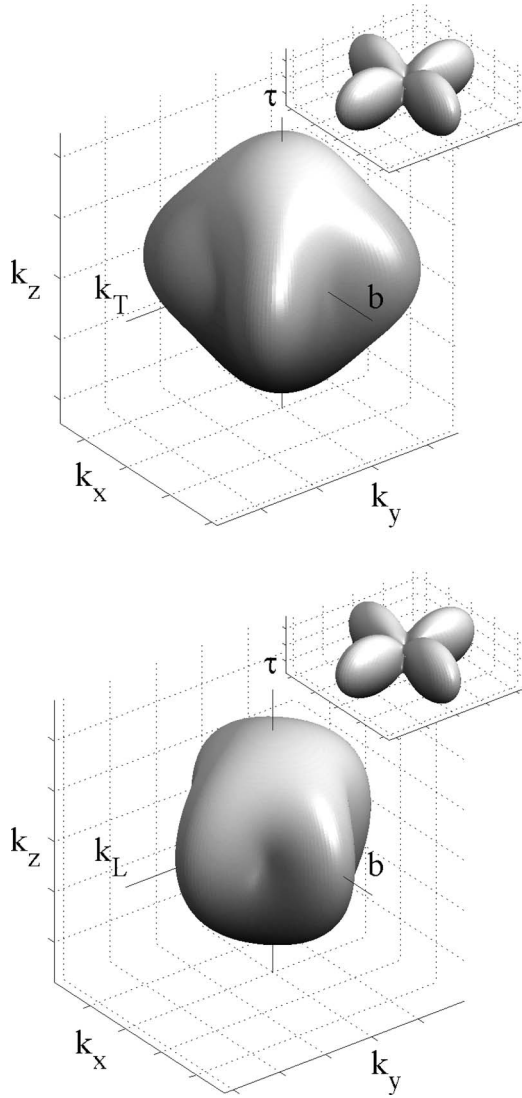


FIG. 3. Modified wave numbers (a) K_T and (b) K_L as a function of the incident wave direction, in a medium made of dislocations segments randomly located but all pointing along the \mathbf{e}_3 direction with Burgers vectors along \mathbf{e}_1 (Fig. 2). The deviation from a spherical shape indicates the anisotropy of the medium. Insets show the change in wave vectors $(K_a - k_a)/k_a$, $a=L, T$. Vectors k_T and k_L indicate the particular incidence considered in the GL model.

$$\alpha_T = \frac{4}{5\pi^6} \frac{\mu b^2 \Lambda L^4 B \omega^2}{c_T \Gamma^2} \left(\frac{1}{1 + (\omega/\omega_m)^2} + \frac{4(3\gamma^5 + 2)}{15\pi^3 \gamma^5} \frac{\rho b^2 L}{c_T B} \omega^2 \frac{1 - (\omega/\omega_m)^2}{[1 + (\omega/\omega_m)^2]^2} \right). \quad (4.3)$$

The above expressions can be further simplified depending on the ratio B/B_c , with $B_c = 2m\omega_1$. Attenuations $\alpha = \alpha_a$ and velocity changes $\Delta v/c \equiv (c_a - v_a)/c_a$ ($a=T, L$) have two typical behaviors.

(i) In the underdamped regime, $B/B_c < 1$ so that ω_m is above the largest considered frequency ω_1 and $\omega/\omega_m \ll 1$. We get

$$\frac{\Delta v_a}{c_a} \approx C_a \frac{\mu b^2}{\Gamma} \Lambda L^2, \quad (4.4)$$

with $C_T = 4/(5\pi^4)$, $C_L = 16/(15\pi^4 \gamma^2)$, and

$$\alpha_a = C'_a \frac{\mu b^2 \Lambda L^4 B \omega^2}{c_a \Gamma^2} \left(1 + C \frac{\rho b^2 L}{c_T B} \omega^2 \right), \quad (4.5)$$

with $C'_T = 4/(5\pi^6)$, $C'_L = 16/(15\pi^6 \gamma^2)$, and $C = 4(3\gamma^5 + 2)/(15\pi^3 \gamma^5)$. The frequency law for the attenuation contains the usual quadratic term^{14–16} and an extra quartic term due to the multiple scattering process that takes energy away from the incident direction, even without any drag. This term can be dominant in the underdamped regime only and appears as a correction to the quadratic term otherwise. Note that the following scaling properties on attenuation and velocity change

$$\alpha \propto L^4, \quad \frac{\Delta v}{c} \propto L^2, \quad (4.6)$$

announced in the GL model¹⁵ and used in experiments^{5,9,10,12,41–43} are recovered. However, because the GL model predicts prefactors C and C' that correspond to a specific (i.e., nonrandom) configuration for scalar waves (see Sec. III), the law must be slightly modified for random configuration in interaction with vector waves, as discussed further in this section.

(ii) In the overdamped regime, attenuations and velocity changes have a frequency law that depends on the frequency range. For $\omega \ll \omega_m < \omega_1$, the frequency laws are the same as in the underdamped regime in Eqs. (4.4)–(4.6) and for $\omega \gg \omega_m$, the frequency laws become

$$\frac{\Delta v_a}{c_a} \approx \pi^4 C_a \mu b^2 \frac{\Gamma}{B^2} \frac{\Lambda}{L^2} \frac{1}{\omega^2}, \quad (4.7)$$

and

$$\alpha_a = \pi^4 C'_a \frac{\mu b^2}{c_a B} \Lambda \left(1 + C \frac{\rho b^2 L}{c_T B} \omega^2 \right). \quad (4.8)$$

These behaviors are illustrated in Fig. 4.

Usual estimates for the drag coefficient B fall around 10^{-5} Pa·s at room temperature, in rough agreement with various estimates $B \approx 10^{-2} \mu b / c_T$ (Refs. 44–46) (this estimation comes from the expression of B above the Debye temperature, $B \approx kT\omega_D^2 / \pi^3 c_T^3$, with k the Boltzmann constant, $\omega_D \approx c_T \pi / b$ the Debye frequency and T the temperature, and taking $\mu b^3 \approx 1$ eV, an estimate valid for most materials). Thus, we have

$$\omega_m \approx 50\pi c_T \frac{b}{L^2}. \quad (4.9)$$

With typical micrometer dislocation lengths L , Burgers vector $b \approx 0.5$ nm, velocities $c_T \approx 3 \times 10^3$ m/s, and frequencies $\omega_m \approx 250$ MHz, well above the typical kHz to MHz frequencies used in many experiments, the simplified Eqs. (4.4) and (4.5) can be used. Care must be exercised, however, when conditions in some recent experiments are reached, such as (i) in the GHz regime of Refs. 32–34, (ii) with the use of

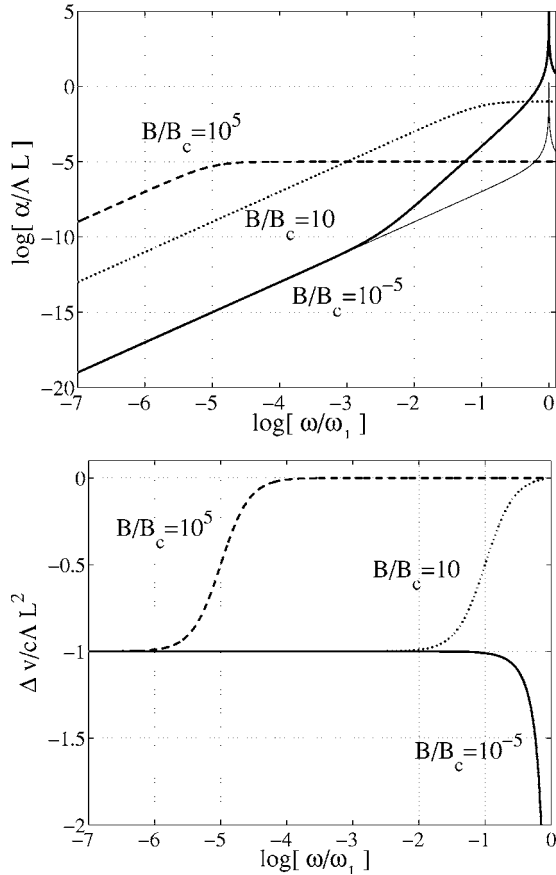


FIG. 4. Typical variations of (a) the attenuation α normalized with ΛL and (b) the velocity change $\Delta v/c$ normalized with ΛL^2 , as a function of $\ln \omega/\omega_1$ for $B/B_c=10^{-5}$ corresponding to the underdamped regime (bold solid line), $B/B_c=10$ corresponding to the weakly overdamped regime (dotted line) and $B/B_c=10^5$ corresponding to the strongly overdamped regime (dotted line). The curve in simple solid line in (a) corresponds to the usual quadratic law, in contrast with the quartic term, dominant in the underdamped regime for ω close to ω_1 .

metal of high purity because the decrease of pinning points increases the L value, and thus decreases ω_m , see for instance the discussion in Ref. 9, (iii) for high temperatures, that cause an increase in B and thus a decrease in ω_m [in that case, Eq. (4.9) is no longer valid], see for instance, Ref. 7.

Expressions similar to Eqs. (4.4) and (4.5) have been widely used in the form proposed in the GL model and rewritten in Ref. 17 as

$$\frac{\Delta v}{c_T} \simeq C \frac{\mu b^2}{\Gamma} \Lambda L^2, \quad (4.10)$$

$$\alpha_a = C' \frac{\mu b^2 \Lambda L^4 B \omega^2}{c_a \Gamma^2}, \quad (4.11)$$

with $C=4\Omega/\pi^4$ and $C'=4\Omega/\pi^6$ issued from Eqs. (3.9) in the low frequency regime where Stern and Granato introduce an ‘‘orientation factor’’ Ω to take into account the fact that the resolved shear stress on the slip systems are smaller than the applied stress. This factor is usually taken equal to

TABLE I. Prefactors for the velocity change and attenuation C, C' from Stern and Granato, and C_a, C'_a , $a=L, T$ from the present study.

C	$4\Omega/\pi^4$	C'	$4\Omega/\pi^6$
C_T	$4/5\pi^4$	C'_T	$4/5\pi^6$
C_L	$16/15\pi^4\gamma^2$	C'_L	$16/15\pi^6\gamma^2$

$\Omega \approx 0.3$.^{3,41} As previously seen, the above expressions are similar, at first order, to our expressions (4.4) and (4.5). However, when quantitative deductions are needed, the discrepancies between our factors C_a and C'_a , $a=L, T$ and the factors in the previous expressions must be studied in more detail. Table I summarizes the differences for both L and T waves.

It appears that, for transverse waves, the empirical value $\Omega \approx 0.3$ reasonably compensates for the discrepancy between the results of GL and our own. In contrast, for longitudinal waves, Ω has to be compared with $4/(15\gamma^2) \approx 1/15$, which is smaller than the usual 0.3 value. However, this is not sufficient to notably modify the results experimentally obtained. For instance, in Ref. 41, the authors measure the attenuation and the velocity change for longitudinal waves propagating in aluminum. Then, they solve the system of Eqs. (4.10) and (4.11) to determine Λ and L . The calculation for L depends on the ratio $C/C' = \pi^2$ which is the same in the GL model as well as in ours. The calculation for Λ , however, depends on the ratio C^2/C' , so that its value must be corrected by a factor 15Ω . With $\Omega=0.32$ taken by the authors, the true Λ is 5 times higher than announced, a discrepancy that is probably not significant.

However, the significant result of our analysis is to give a possible explanation to the difference between longitudinal and transverse attenuations first observed in Ref. 3, as will be seen in the next section.

B. RUS and EMAR experiments

The basic idea of resonant ultrasound spectroscopy (RUS) is to record the spectrum of resonance peaks of a suitably excited sample. For a detailed description of the theory and application of RUS, see Ref. 47. The resonance frequencies ω^r are used to infer elastic moduli while the quality factor follows from the measurements of the resonant peak widths through $Q^{-1} = \Delta\omega/\omega^r$. An ad-hoc treatment of the inverse problem allows for the computation of all elastic constants as necessitated by the symmetry of the sample. Among the elastic constants, c_{11} is related to the longitudinal mode and c_{44} to the transverse modes. In addition, the shear (μ) and longitudinal ($\lambda+2\mu$) moduli have been calculated for copper single crystals in Ref. 9.

Electromagnetic acoustic resonance (EMAR) experiments are a variant of RUS using electromagnetic acoustic transducers (EMAT). EMAT generate and receive ultrasonic waves through electromagnetic effects, avoiding the energy losses that occur with contact measurements. In EMAR, attenuation can be measured as the exponent in the exponentially time decreasing response of the sample to a burst sig-

TABLE II. Internal friction measured by EMAR and RUS for resonances associated with longitudinal waves (Q_{11}) and shear waves (Q_{44}). The right-hand side of the table gives the shear and longitudinal internal friction coefficients Q_T^{-1} and Q_L^{-1} from Ref. 8. The last column gives the value Q_T^{-1}/Q_L^{-1} to be compared with $3\gamma/4$ from Eq. (4.13) with $\gamma=2$ for copper (Ref. 9). We also estimate $\gamma=2$ for LiNbO₃.

	$Q_{11}^{-1}-Q_L^{-1}$	$Q_{44}^{-1}-Q_T^{-1}$	Q_T^{-1}/Q_L^{-1}
Polycrystalline copper (from Ref. 3) using RUS	0.9×10^{-3}	1.46×10^{-3}	1.62
LiNbO ₃ (from Ref. 11) using RUS	2.2×10^{-5}	3.7×10^{-5}	1.68
Copper single crystal (from Ref. 8) using RUS	$1.74-1.84 \times 10^{-3}$	$2.46-2.57 \times 10^{-3}$	1.41-1.40
Copper single crystal (from Ref. 8) using EMAR	$1.14-1.34 \times 10^{-3}$	$2.59-2.83 \times 10^{-3}$	2.28-2.11

nal at resonance frequency (ringdown curve).^{4,5,8,9,12} If α^t is the exponential coefficient, the quality factor is deduced for each mode of vibration through $Q^{-1}=2\alpha^t/\omega^r$ (the temporal attenuation is simply related to the spatial attenuation α through $\alpha=\alpha^t/c$). The resonant frequencies are typically of a few tenths of MHz, so that these experiments are in the regime $\omega \ll \omega_m$, and we expect to have

$$Q_L^{-1} = \frac{32}{15\pi^2} \frac{1}{\gamma^4} \frac{\rho b^2}{m} \Lambda \frac{c_L^2 B \omega_L^r}{m \omega_1^4} \approx \frac{128}{15\pi^4} \frac{1}{\gamma^2} \frac{\Lambda B L^4 \omega_L^r}{\rho b^2 c_T^2},$$

$$Q_T^{-1} = \frac{8}{5\pi^2} \frac{\rho b^2}{m} \Lambda \frac{c_T^2 B \omega_T^r}{m \omega_1^4} \approx \frac{32}{5\pi^4} \frac{\Lambda B L^4 \omega_T^r}{\rho b^2 c_T^2}, \quad (4.12)$$

where ω_L^r , ω_T^r , denote the resonant frequencies for longitudinal and transverse modes, respectively. The second equalities in both Eqs. (4.12) are obtained with $\omega_1 = \sqrt{\Gamma/m}\pi/L$ and Γ , given in Eq. (2.3) in Paper I, roughly equal to $\rho b^2 c_T^2 / (2\pi)$. From Eqs. (4.12), we expect

$$\frac{Q_T^{-1}}{Q_L^{-1}} \approx \frac{3}{4} \gamma \sim 1.30 - 1.56, \quad (4.13)$$

where we have taken $\omega_T^r/\omega_L^r = c_T/c_L \gamma^{-1}$ and γ ranging from 1.7 to 2 (typical Poisson's ratio range from 0.25 to 0.35). Various measurements of the quality factors Q_{ii} associated to the c_{ii} for $i=1, 4$ can be found in Refs. 3,8,9,11. In Ref. 9, the shear and longitudinal quality factors Q_L^{-1} and Q_T^{-1} , corresponding to the shear and longitudinal moduli, have been calculated. The results are summarized in Table II, where it can be seen that the ratio Q_T^{-1}/Q_L^{-1} obtained with RUS reasonably agree with the values found in Eq. (4.13) while EMAR method gives a higher ratio.

Finally, experimental values for polycrystalline copper can be found in Ref. 3, $\rho=8.9 \times 10^3$ kg m⁻³, $c_T=2150$ m/s, and $\Lambda \sim 10^{10}$ m⁻² and values for LiNbO₃ can be found in

Refs. 32-34 and 11, $\rho=4.6 \times 10^3$ K g m⁻³, $c_T=3758$ m/s and $\Lambda \sim 2 \times 10^8$ m⁻². In both cases, expressions (4.12) with values of Q^{-1} in Table I give $L \sim 10$ μ m.

V. CONCLUDING REMARKS

We have worked out a full theory of vector elastic waves in an elastic medium interacting with an ensemble of randomly distributed and oriented dislocation segments that takes into account the vector nature of the interaction as well. This theory shows that the widely used Granato and Lücke model is a special case, in which only a single polarization of the waves is allowed, as well as a uniform orientation for the dislocations. Our more general theory provides different numbers for wave velocity change and attenuation coefficient depending on wave polarization (longitudinal or transverse), as observed in experiments. Further work is needed to determine if the scattering by dislocations can be considered as the dominant factor among the different mechanisms that generally affect the wave propagation. However, the comparison presented in this paper suggests that it is a good candidate to explain these experimental results.

ACKNOWLEDGMENTS

This work has been supported by ECOS Contract No. C04E01 and by FONDAP Grant No. 11980002. One of the authors (F.B.) thanks Fondecyt project 1030556. Two of the authors (A.M. and V.P.) are pleased to thank Erik Bitzek for fruitful discussions.

APPENDIX A: ON THE EULER ANGLES AND AVERAGES OF ROTATION

The rotation matrix $\mathbf{R} \equiv \mathbf{R}(\mathbf{e}_3, \theta)\mathbf{R}(\mathbf{e}_2, \varphi)\mathbf{R}(\mathbf{e}_1, \xi)$,

$$\mathbf{R} = \begin{pmatrix} \cos \varphi \cos \theta & -\sin \theta \cos \xi - \sin \varphi \cos \theta \sin \xi & \sin \theta \sin \xi - \sin \varphi \cos \theta \cos \xi \\ \cos \varphi \sin \theta & \cos \theta \cos \xi - \sin \varphi \sin \theta \sin \xi & -\cos \theta \sin \xi - \sin \varphi \sin \theta \cos \xi \\ \sin \varphi & \cos \varphi \sin \xi & \cos \varphi \cos \xi \end{pmatrix} \quad (A1)$$

defined with the Euler angles (θ, φ, ξ) , is the matrix that takes the basis $(\mathbf{e}_1, \mathbf{e}_2, \mathbf{e}_3)$ to $(\mathbf{e}_r, \mathbf{e}_\xi, \mathbf{e}_r \times \mathbf{e}_\xi)$ (see Fig. 10 in Paper I).

We define the average of a function $f(\theta, \varphi, \xi)$ over the Euler angles as

$$\langle f \rangle = \frac{1}{8\pi^2} \int_0^{2\pi} d\theta \int_{-\pi/2}^{\pi/2} \cos \varphi d\varphi \int_0^{2\pi} d\xi f(\theta, \varphi, \xi). \quad (\text{A2})$$

The following tabulated averages can be found in Ref. 48:

$$\begin{aligned} \langle \mathbf{R}_{Fi} \mathbf{R}_{Fj} \mathbf{R}_{Gk} \mathbf{R}_{Gl} \rangle &= \frac{4\delta_{ij}\delta_{kl} - \delta_{ik}\delta_{jl} - \delta_{il}\delta_{jk}}{30}, \\ \langle \mathbf{R}_{Fi} \mathbf{R}_{Fj} \mathbf{R}_{Fk} \mathbf{R}_{Fl} \rangle &= \frac{\delta_{ij}\delta_{kl} + \delta_{ik}\delta_{jl} + \delta_{il}\delta_{jk}}{15}, \\ \langle \mathbf{R}_{Fi} \mathbf{R}_{Fj} \rangle &= \frac{\delta_{ij}}{3}. \end{aligned} \quad (\text{A3})$$

Note that if the average is done on the spherical angles (θ, φ) , $\langle f \rangle = (1/4\pi) \int \cos \varphi d\theta d\varphi f(\theta, \varphi)$ it is sufficient to use the preceding properties, with a factor 2π because of the integral over ξ .

APPENDIX B: THE GREEN FUNCTION IN FREE SPACE

The Green function free space G^0 satisfies

$$\rho \frac{\partial^2}{\partial t^2} G_{im}^0(\mathbf{x}, t) - c_{ijkl} \frac{\partial^2}{\partial x_j \partial x_l} G_{km}^0(\mathbf{x}, t) = \delta(\mathbf{x}) \delta(t) \delta_{im}. \quad (\text{B1})$$

In Fourier and frequency space, we get $G^{0-1}(\mathbf{k}, \omega)$

$$G_{ik}^{0-1}(\mathbf{k}, \omega) = (-\rho\omega^2 + \mu k^2) \delta_{ik} + (\lambda + \mu) k_i k_k. \quad (\text{B2})$$

Using $\rho c_L^2 = \lambda + 2\mu$, $\rho c_T^2 = \mu$ and with $\mathbf{P}_{\hat{\mathbf{k}}} \equiv \hat{\mathbf{k}} \hat{\mathbf{k}}$ the projector on \mathbf{k} , it can be written as

$$G^{0-1}(\mathbf{k}, \omega) = \rho c_T^2 (k^2 - k_T^2) (1 - \mathbf{P}_{\hat{\mathbf{k}}}) + \rho c_L^2 (k^2 - k_L^2) \mathbf{P}_{\hat{\mathbf{k}}}, \quad (\text{B3})$$

and we get also

$$G^0(\mathbf{k}, \omega) = \frac{1}{\rho c_T^2 (k^2 - k_T^2)} (1 - \mathbf{P}_{\hat{\mathbf{k}}}) + \frac{1}{\rho c_L^2 (k^2 - k_L^2)} \mathbf{P}_{\hat{\mathbf{k}}}. \quad (\text{B4})$$

APPENDIX C: TECHNICAL CALCULATIONS FOR THE DERIVATION OF THE MASS OPERATOR

The derivation of the mass operator Σ gives the modified Green tensor $\langle G \rangle$ through Eq. (2.14). The poles of the modified Green tensor are the effective wave numbers K_c ($c=L, T$) that characterize the coherent wave propagation in an effective medium defined as the average over all random distribution of dislocation segments. For weak scattering, Σ can be developed in powers of the potential V [appearing in

Eq. (2.13) and assumed to be small]. At first and second orders, the relations between Σ and V are given by

$$\Sigma_{ik}^{(1)}(\mathbf{k}) = n \int d\mathbf{x} d\mathbf{C} e^{-i\mathbf{k}\mathbf{x}} V_{ik}(\mathbf{x}) e^{i\mathbf{k}\mathbf{x}},$$

$$\Sigma_{ij}^{(2)}(\mathbf{k}) = n \int d\mathbf{x} d\mathbf{x}' d\mathbf{C} e^{-i\mathbf{k}\mathbf{x}} V_{in}(\mathbf{x}) G_{nl}^0(\mathbf{x} - \mathbf{x}') V_{lj}(\mathbf{x}') e^{i\mathbf{k}\mathbf{x}'}, \quad (\text{C1})$$

where $G_{nl}^0(\mathbf{x} - \mathbf{x}')$ means $G_{nl}^0(\mathbf{x} - \mathbf{x}', \omega)$. We provide below the derivation of the two first orders of the mass operator. The integration over \mathbf{C} indicates the average over all realizations of V , each realization includes the positions of the centers \mathbf{X}_0 and the orientations of the dislocation segments, and the Burgers vectors. For the sake of simplicity, we consider in the following calculations only the average over all vectors \mathbf{X}_0 and over all orientations of the dislocation segments and Burgers vectors. It would be sufficient to replace b^2 by $\langle b^2 \rangle$ in the final result to account for the other averages. Note that the average over the orientations of the dislocation segments and associated Burgers vector is simply obtained by averaging over all possible orientations of $(\mathbf{t}, \mathbf{n}, \boldsymbol{\tau}) = \mathbf{R}(\mathbf{e}_1, \mathbf{e}_2, \mathbf{e}_3)$, with \mathbf{R} defined in Eq. (A1).

1. Derivation of the mass operator at first order

The first order is easily obtained. Using the expression of the potential Eq. (2.11) in the first relation of Eq. (C1), we get

$$\begin{aligned} \Sigma_{ik}^{(1)}(\mathbf{k}) &= \frac{8}{\pi^2} \frac{(\mu b)^2 S(\omega)}{m \omega^2} nL \int d\mathbf{x} d\mathbf{C} e^{-i\mathbf{k}\mathbf{x}} \mathbf{M}_{ij} \\ &\quad \times \frac{\partial}{\partial x_j} \delta(\mathbf{x} - \mathbf{X}_0) \mathbf{M}_{lk} \frac{\partial}{\partial x_l} \Big|_{\mathbf{x}=\mathbf{X}_0} e^{i\mathbf{k}\mathbf{x}} \\ &= -\frac{8}{\pi^2} \frac{(\mu b)^2 S(\omega)}{m \omega^2} nL \int d\mathbf{x} d\mathbf{C} \frac{\partial}{\partial x_j} e^{-i\mathbf{k}\mathbf{x}} \mathbf{M}_{ij} \\ &\quad \times \delta(\mathbf{x} - \mathbf{X}_0) \mathbf{M}_{lk} k_l e^{i\mathbf{k}\mathbf{X}_0} \\ &= -\frac{8}{\pi^2} \frac{(\mu b)^2 S(\omega)}{m \omega^2} nL \int d\mathbf{C} \mathbf{M}_{ij} \mathbf{M}_{lk} k_j k_l. \end{aligned} \quad (\text{C2})$$

The integral in $\Sigma^{(1)}$ is an average of the tensor $\mathbf{M} \hat{\mathbf{k}} \hat{\mathbf{k}} \mathbf{M}$ with $\mathbf{M}_{ij} = n_i t_j + t_i n_j$ over all possible orientations of \mathbf{t} and \mathbf{n} . Letting $t_i = R_{i1}$ and $n_i = R_{i2}$, we get

$$\begin{aligned} [\mathbf{M} \hat{\mathbf{k}} \hat{\mathbf{k}} \mathbf{M}]_{ij} &= (n_i t_m + t_i n_m) (n_n t_j + t_n n_j) \hat{k}_m \hat{k}_n \\ &= (R_{i2} R_{n2} R_{m1} R_{j1} + R_{i2} R_{j2} R_{n1} R_{m1} \\ &\quad + R_{i1} R_{j1} R_{n2} R_{m2} \\ &\quad + R_{j2} R_{m2} R_{n1} R_{i1}) \hat{k}_m \hat{k}_n. \end{aligned} \quad (\text{C3})$$

Using the first and the second relations in Eqns. (A3), we obtain

$$\begin{aligned} \langle [\mathbf{M} \hat{\mathbf{k}} \hat{\mathbf{k}} \mathbf{M}]_{ij} \rangle &= \frac{2}{30} (4\delta_{in} \delta_{jm} - \delta_{ij} \delta_{mn} - \delta_{im} \delta_{jn} + 4\delta_{ij} \delta_{mn} - \delta_{in} \delta_{jm} \\ &\quad - \delta_{im} \delta_{jn}) \hat{k}_m \hat{k}_n = \frac{1}{15} (\hat{k}_i \hat{k}_j + 3\delta_{ij}). \end{aligned} \quad (\text{C4})$$

Finally, we get

$$\Sigma_{ik}^{(1)}(\mathbf{k}) = -\frac{8}{15\pi^2} \frac{\rho b^2 S(\omega)}{m \omega^2} nL \rho c_T^4 k^2 (\hat{k}_i \hat{k}_k + 3\delta_{ik}). \quad (\text{C5})$$

This equation is the first relation of Eqs. (2.16).

2. Derivation of the mass operator at second order

Using the expression of the potential, Eq. (2.11), in the second relation of Eq. (C1), we get

$$\begin{aligned} \Sigma_{ij}^{(2)}(\mathbf{k}) &= n \left(\frac{8}{\pi^2} \frac{(\mu b)^2 S(\omega)}{m \omega^2} L \right)^2 \\ &\times \int d\mathbf{x} d\mathbf{x}' d\mathbf{C} e^{-i\mathbf{k}\mathbf{x}} \mathbf{M}_{ik} \frac{\partial}{\partial x_k} \delta(\mathbf{x} - \mathbf{X}_0) \mathbf{M}_{mn} \\ &\times \frac{\partial}{\partial x_m} \Big|_{\mathbf{x}=\mathbf{X}_0} G_{nl}^0(\mathbf{x} - \mathbf{x}') \mathbf{M}_{lp} \frac{\partial}{\partial x'_p} \delta(\mathbf{x}' - \mathbf{X}_0) \mathbf{M}_{qj} \\ &\times \frac{\partial}{\partial x'_q} \Big|_{\mathbf{x}'=\mathbf{X}_0} e^{i\mathbf{k}\mathbf{x}'}. \end{aligned} \quad (\text{C6})$$

The Green function is written as $G^0(\mathbf{x}) = 1/(2\pi)^3 \int d\mathbf{q} G^0(\mathbf{q}) e^{i\mathbf{q}\mathbf{x}}$, so we get

$$\begin{aligned} \Sigma_{ij}^{(2)}(\mathbf{k}) &= \frac{8}{\pi^7} \frac{(\mu b)^4 S^2(\omega)}{m^2 \omega^4} nL^2 \int d\mathbf{x} d\mathbf{x}' d\mathbf{C} d\mathbf{q} e^{-i\mathbf{k}\mathbf{x}} \mathbf{M}_{ik} \\ &\times \frac{\partial}{\partial x_k} \delta(\mathbf{x} - \mathbf{X}_0) \mathbf{M}_{mn} (iq_m) G_{nl}^0(\mathbf{q}) e^{i\mathbf{q}(\mathbf{X}_0 - \mathbf{x}')} \mathbf{M}_{lp} \\ &\times \frac{\partial}{\partial x'_p} \delta(\mathbf{x}' - \mathbf{X}_0) \mathbf{M}_{qj} (ik_q) e^{i\mathbf{k}\mathbf{x}_0} \\ &= \frac{8}{\pi^7} \frac{(\mu b)^4 S^2(\omega)}{m^2 \omega^4} nL^2 \int d\mathbf{x} d\mathbf{x}' d\mathbf{C} d\mathbf{q} (ik_k) e^{-i\mathbf{k}\mathbf{X}_0} \mathbf{M}_{ik} \\ &\times \delta(\mathbf{x} - \mathbf{X}_0) \mathbf{M}_{mn} \times (iq_m) G_{nl}^0(\mathbf{q}) (iq_p) e^{i\mathbf{q}(\mathbf{X}_0 - \mathbf{X}_0)} \mathbf{M}_{lp} \\ &\times \delta(\mathbf{x}' - \mathbf{X}_0) \mathbf{M}_{qj} (ik_q) e^{i\mathbf{k}\mathbf{X}_0} \\ &= \frac{8}{\pi^7} \frac{(\mu b)^4 S^2(\omega)}{m^2 \omega^4} nL^2 I_{lmp} \int d\mathbf{C} \mathbf{M}_{ik} \mathbf{M}_{mn} \mathbf{M}_{lp} \mathbf{M}_{qj} k_q k_k, \end{aligned} \quad (\text{C7})$$

where

$$I_{lmp} \equiv \int d\mathbf{q} G_{nl}^0(\mathbf{q}) q_p q_m. \quad (\text{C8})$$

The Green function is given in Appendix B of the form $G^0(\mathbf{k}) = g_T(k)(1 - \mathbf{P}_{\hat{\mathbf{k}}}) + g_L(k)\mathbf{P}_{\hat{\mathbf{k}}}$, with $g_T(k) = 1/[\rho c_T^2(k^2 - k_T^2)]$, $g_L(k) = 1/[\rho c_L^2(k^2 - k_L^2)]$. Denoting $g(k) = g_L(k) - g_T(k)$, we have $I_{lmp} = \int d\mathbf{q} [g_T(q)\delta_{nl} + g(q)\hat{q}_n \hat{q}_l] q_p q_m = \int d\mathbf{q} q^4 g_T(q) \times \int d\hat{\mathbf{q}} \hat{q}_p \hat{q}_m \delta_{nl} + \int d\mathbf{q} q^4 g(q) \int d\hat{\mathbf{q}} \hat{q}_n \hat{q}_l \hat{q}_p \hat{q}_m$.

The integrals over the spherical angles of $\hat{\mathbf{q}}$ are known (see for instance Appendix A) $\int d\hat{\mathbf{q}} \hat{q}_p \hat{q}_m = 4\pi/3 \delta_{mp}$ and $\int d\hat{\mathbf{q}} \hat{q}_n \hat{q}_l \hat{q}_p \hat{q}_m = 4\pi/15 (\delta_{lm}\delta_{np} + \delta_{ln}\delta_{mp} + \delta_{lp}\delta_{mn})$.

The integrals over the modulus q are divergent at high wave numbers and they are regularized introducing a cutoff

function at small lengths $q > 1/b$, since b is the smallest length available for the validity of continuum elasticity. In any case we only need the (finite) imaginary part of the integral. The real part of the integral, that depends on the form of the cutoff function is not considered here since it is a higher order term in the change of velocity and can be neglected. In contrast, the imaginary part of the mass operator at order two must be considered since it is the dominant term of the attenuation for vanishing drag. Thus, we have $\text{Im}[\int d\mathbf{q} q^4 g_T(q)] = \pi k_T^3 / 2\rho c_T^2$, $\text{Im}[\int d\mathbf{q} q^4 g(q)] = \pi(k_L^3 / 2\rho c_L^2 - k_T^3 / 2\rho c_T^2)$, and

$$\begin{aligned} \text{Im}(I_{lmp}) &= \frac{2\pi^2}{15} \frac{\omega^3}{\rho c_T^5} \left(5\delta_{mp}\delta_{nl} + \frac{1-\gamma^5}{\gamma^5} (\delta_{lm}\delta_{np} + \delta_{ln}\delta_{mp} \right. \\ &\quad \left. + \delta_{lp}\delta_{mn}) \right), \end{aligned} \quad (\text{C9})$$

with $\gamma \equiv c_L/c_T$. This is now used in Eq. (C7) to get the imaginary part of $\Sigma^{(2)}$,

$$\begin{aligned} \text{Im}[\Sigma_{ij}^{(2)}(\mathbf{k})] &= \frac{16}{15\pi^5} \left(\frac{\rho b^2}{m} \right)^2 \frac{S^2(\omega)}{\omega} \rho c_T^3 nL^2 \int d\mathbf{C} \left(5\mathbf{M}_{mn}\mathbf{M}_{nm} \right. \\ &\quad \left. + \frac{1-\gamma^5}{\gamma^5} (\mathbf{M}_{mn}\mathbf{M}_{mn} + \mathbf{M}_{nm}\mathbf{M}_{nm} \right. \\ &\quad \left. + \mathbf{M}_{mm}\mathbf{M}_{ll}) \right) \mathbf{M}_{ik}\mathbf{M}_{qj} k_q k_k. \end{aligned} \quad (\text{C10})$$

With \mathbf{M} defined in Eq. (2.5) in Paper I and using $t_m n_m = 0$, $t_m t_m = n_m n_m = 1$, it is easy to see that $\mathbf{M}_{mm} = 0$ and $\mathbf{M}_{mn}\mathbf{M}_{nm} = \mathbf{M}_{mn}\mathbf{M}_{nm} = 2$. We thus have

$$\begin{aligned} \text{Im}[\Sigma_{ij}^{(2)}(\mathbf{k})] &= \frac{32}{15\pi^5} \frac{3\gamma^5 + 2}{\gamma^5} \left(\frac{\rho b^2}{m} \right)^2 \frac{S^2(\omega)}{\omega} \rho c_T^3 nL^2 \\ &\quad \times \int d\mathbf{C} \mathbf{M}_{ik}\mathbf{M}_{qj} k_q k_k, \end{aligned} \quad (\text{C11})$$

where the integral has been evaluated in Eqn. (C4). Finally, we obtain

$$\begin{aligned} \text{Im}[\Sigma^{(2)}(\mathbf{k})] &= \frac{32}{225\pi^5} \frac{3\gamma^5 + 2}{\gamma^5} \left(\frac{\rho b^2}{m} \right)^2 \frac{S^2(\omega)}{\omega} \rho c_T^3 nL^2 k^2 (\hat{\mathbf{k}}' \hat{\mathbf{k}} \\ &\quad + 3\mathbf{1}). \end{aligned} \quad (\text{C12})$$

This equation is the second relation of Eqs. (2.16).

APPENDIX D: FOLDY'S APPROACH

1. The formalism for 3D polarized waves

Foldy's approach to coherent wave propagation consists in writing the total velocity field as the sum of the incident wave plus the scattered waves

$$\mathbf{v}(\mathbf{x}) = \mathbf{v}^{\text{inc}}(\mathbf{x}) + \sum_{i=1}^N F(\mathbf{x}, \mathbf{X}_i) \mathbf{v}(\mathbf{X}_i), \quad (\text{D1})$$

where $F(\mathbf{x}, \mathbf{X}_i) \mathbf{v}(\mathbf{X}_i)$ is the contribution of a scatterer located at \mathbf{X}_i and receiving the wave $\mathbf{v}(\mathbf{X}_i)$. The function F is iden-

tified as the response of an individual scatterer $F(\mathbf{x}, \mathbf{X}) = f(\theta, \varphi) e^{ik|\mathbf{x}-\mathbf{X}|}/|\mathbf{x}-\mathbf{X}|$, with f depending on the parameters \mathbf{C} characteristic of the scatterer. By taking the average over all realizations of the positions \mathbf{X} of the scatterers and of the parameters \mathbf{C} , we get

$$\langle \mathbf{v} \rangle(\mathbf{x}) = v^{\text{inc}}(\mathbf{x}) + n \int d\mathbf{X} \langle f \rangle_{\mathbf{c}}(\theta, \varphi) \frac{e^{ik|\mathbf{x}-\mathbf{X}|}}{|\mathbf{x}-\mathbf{X}|} \langle \mathbf{v} \rangle(\mathbf{X}). \quad (\text{D2})$$

In the most general case of three directions of polarization, the solution for $\langle \mathbf{v} \rangle$ is assumed to be of the form $\langle \mathbf{v} \rangle(x_1) = \sum_{m=1}^3 B_m e^{iK_m x_1} \mathbf{e}_m$ for an incident wave of the form $\mathbf{v}^{\text{inc}}(x_1) = \sum_{m=1}^3 A_m e^{iK_m x_1} \mathbf{e}_m$, where B_m and K_m must be determined as solutions of

$$\begin{aligned} B_m e^{iK_m x_1} &= A_m e^{iK_m x_1} + n \sum_j B_j \int d\mathbf{X} \frac{\langle f_{mj} \rangle_{\mathbf{c}}(\theta, \varphi) e^{ik_j |\mathbf{x}-\mathbf{X}|}}{|\mathbf{x}-\mathbf{X}|} e^{iK_j x_1} \\ &= A_m e^{iK_m x_1} + n \sum_j B_j \frac{2\pi}{k_j} \langle f_{mj} \rangle_{\mathbf{c}}(0, 0) \frac{e^{iK_j x_1} - e^{iK_m x_1}}{(K_j - k_j)}, \end{aligned} \quad (\text{D3})$$

that can be rearranged as

$$\begin{aligned} e^{iK_m x_1} B_m \left(1 - n \frac{2\pi \langle f_{mm} \rangle_{\mathbf{c}}(0, 0)}{k_m (K_j - k_j)} \right) \\ - e^{iK_m x_1} \left(A_m - B_m n \frac{2\pi \langle f_{mm} \rangle_{\mathbf{c}}(0, 0)}{k_m (K_j - k_j)} \right) \\ - n \sum_{j \neq m} B_j \frac{2\pi}{k_j} \langle f_{mj} \rangle_{\mathbf{c}}(0, 0) \frac{e^{iK_j x_1} - e^{iK_m x_1}}{(K_j - k_j)} = 0. \end{aligned} \quad (\text{D4})$$

Note that the above system has no solution if $\langle f_{mj} \rangle_{j \neq m} \neq 0$, that is if there exists mode conversion in average over the realizations. Alternatively, if there is no conversion in average (over \mathbf{C}), the solution is $B_m = A_m$ and

$$K_m = k_m + n \frac{2\pi}{k_m} \langle f_{mm} \rangle_{\mathbf{c}}(0, 0), \quad (\text{D5})$$

2. Derivation of the modified wave numbers

In our case, the Foldy approach can be applied for an incident wave propagating along a fixed direction $\hat{\mathbf{k}}_0$ with the conventions of Paper I, the average being done over all orientations of the dislocation segments and Burgers vectors. We note $\mathcal{E}_0 = (\hat{\mathbf{k}}_0, \hat{\mathbf{y}}_0, \hat{\mathbf{k}}_0 \times \hat{\mathbf{y}}_0)$ the basis obtained from $\mathcal{E} = (\mathbf{e}_1, \mathbf{e}_2, \mathbf{e}_3)$ by the rotation \mathbf{R}_0 , and $\mathcal{E}_{\hat{\mathbf{x}}} = (\hat{\mathbf{x}}, \hat{\mathbf{y}}, \hat{\mathbf{x}} \times \hat{\mathbf{y}})$ the basis obtained from \mathcal{E} by the rotation \mathbf{R} .

In \mathcal{E}_0 , we get

$$\begin{aligned} \mathbf{v}^{\text{inc}} &= \begin{pmatrix} A_L e^{ik_L \hat{\mathbf{k}}_0 \cdot \mathbf{x}} \\ A_T e^{ik_T \hat{\mathbf{k}}_0 \cdot \mathbf{x}} \\ 0 \end{pmatrix}_{|\mathcal{E}_0}, \quad \mathbf{v}^s = {}^t \mathbf{R} \mathbf{R}_0 \begin{pmatrix} v_L^s \\ v_T^s \\ 0 \end{pmatrix}_{|\mathcal{E}_0}, \\ \mathbf{b} &= b \begin{pmatrix} \mathbf{R}_{0,11} \\ \mathbf{R}_{0,12} \\ \mathbf{R}_{0,13} \end{pmatrix}_{|\mathcal{E}_0}, \end{aligned} \quad (\text{D6})$$

where $v_L^s = [f_{LL}(\hat{\mathbf{x}})A_L + f_{LT}(\hat{\mathbf{x}})A_T](e^{ik_L x}/x)$ and $v_T^s = [f_{TL}(\hat{\mathbf{x}})A_L + f_{TT}(\hat{\mathbf{x}})A_T](e^{ik_T x}/x)$ have been calculated previously. In this basis, \mathbf{b} is a vector with variable direction while the incident wave is fixed. The expression of \mathbf{v}^s in \mathcal{E}_0 is quite complicated. This is why we have not expressed the scattering functions in that basis, even if it is a natural basis to give the scattering functions.

However, in the forward direction, we have ${}^t \mathbf{R} \mathbf{R}_0 \mathbf{R}(\mathbf{e}_1, \xi - \xi_0)$. Remember that ξ is a function of θ and $\varphi[\xi(\theta, \varphi) = \tan^{-1}(\sin \varphi \tan 2\theta)]$, and the forward direction corresponds to $\xi(\theta_0, \varphi_0)$. \mathbf{v}^s takes thus a simpler form in that direction

$$\mathbf{v}^s(\theta_0, \varphi_0) = \begin{pmatrix} v_L^s(\theta_0, \varphi_0) \\ v_T^s(\theta_0, \varphi_0) \cos(\xi - \xi_0) \\ v_T^s(\theta_0, \varphi_0) \sin(\xi - \xi_0) \end{pmatrix}. \quad (\text{D7})$$

This allows us to identify the scattering functions as they appear in Eqs. (D3)–(D5) [but where $f_{mj}(0, 0)$ are replaced here by $f_{mj}(\theta_0, \varphi_0)$ since the direction (θ_0, φ_0) corresponds to the forward direction]. $f_{11}(\theta_0, \varphi_0) = f_{LL}(\theta_0, \varphi_0)$, $f_{12}(\theta_0, \varphi_0) = f_{LT}(\theta_0, \varphi_0)$, $f_{21} = f_{TL}(\theta_0, \varphi_0) \cos(\xi - \xi_0)$, $f_{22} = f_{TT}(\theta_0, \varphi_0) \times \cos(\xi - \xi_0)$, $f_{31} = f_{TL}(\theta_0, \varphi_0) \sin(\xi - \xi_0)$, $f_{32} = f_{TT}(\theta_0, \varphi_0) \sin(\xi - \xi_0)$, and $f_{33}(\theta_0, \varphi_0) = 0$. We now must perform the average

$$\begin{aligned} &\begin{pmatrix} \langle f_{11} \rangle(\theta_0, \varphi_0) & \langle f_{12} \rangle(\theta_0, \varphi_0) & \langle f_{13} \rangle(\theta_0, \varphi_0) \\ \langle f_{21} \rangle(\theta_0, \varphi_0) & \langle f_{22} \rangle(\theta_0, \varphi_0) & \langle f_{23} \rangle(\theta_0, \varphi_0) \\ \langle f_{31} \rangle(\theta_0, \varphi_0) & \langle f_{32} \rangle(\theta_0, \varphi_0) & \langle f_{33} \rangle(\theta_0, \varphi_0) \end{pmatrix} \\ &= -\frac{2}{\pi^3} \left(\frac{\rho b^2}{m} \right) LS(\omega) \begin{pmatrix} \frac{4\gamma^4}{15} & 0 & 0 \\ 0 & \frac{1}{5} & 0 \\ 0 & 0 & 0 \end{pmatrix}. \end{aligned} \quad (\text{D8})$$

There is no coherent wave in the third direction since we have assumed no incident wave in that direction. As the scattering amplitudes have been calculated in the first Born approximation, this result corresponds to the result obtained using the mass operator at first order only. Using (D8) in (D5) reproduces the leading order term in (2.17)

APPENDIX E: DERIVATION OF THE INTEGRAL REPRESENTATION OF THE STRESS AS USED IN THE GL MODEL

To find the wave equation for the stress σ with a source term as used by Granato and Lücke in Eqs. (3.1), we start from the integral representation of Mura⁴⁰ [its Eq. (18)] for the strain tensor β_{nm} ,

$$\begin{aligned} \beta_{nm}(\mathbf{x}, t) = & \int \int_{\mathcal{L}} dt' ds \epsilon_{njh} c_{ijkl} \frac{\partial}{\partial x_l} G_{km}^0(\mathbf{x} - \mathbf{X}, t - t') b_i \tau_h(s, t') \\ & + \int \int_{\mathcal{L}} dt' ds \rho \frac{\partial}{\partial t} G_{im}^0(\mathbf{x} - \mathbf{X}, t - t') b_i \epsilon_{nlh} \dot{X}_l \tau_h. \end{aligned} \quad (\text{E1})$$

We wish to show that the first term on the right-hand side, call it A , does not contribute in the far field. Suppressing indices for ease of understanding, we have

$$A(\mathbf{x}, t) \sim \mu b \int \int_{\mathcal{L}} dt' ds \mathbf{X}'(s, t') \nabla G^0. \quad (\text{E2})$$

Since we are interested only in the far field (distances large compared to dislocation length as well as wavelength), the relevant terms in G^0 are a linear combination of terms of the form

$$G^0 \sim \frac{1}{|\mathbf{x}|} \delta\left(t - t' - \frac{1}{c} |\mathbf{x} - \mathbf{X}(t')|\right)$$

and, still in the far field,

$$\nabla G^0 \sim \frac{\hat{\mathbf{x}}}{c|\mathbf{x}|} \delta'\left(t - t' - \frac{1}{c} |\mathbf{x} - \mathbf{X}(t')|\right),$$

where $\delta' = d\delta/dt$. Substituting into Eq. (E2) we get, in the far field,

$$A(\mathbf{x}, t) \sim \mu b \frac{1}{|\mathbf{x}|} \frac{d}{dt} \int_{\mathcal{L}} ds \mathbf{X}'(s, t_{\text{ret}}),$$

but $\int_{\mathcal{L}} ds \mathbf{X}'(s, t)$ is a constant vector (extremities are fixed points) so that the time derivative vanishes and A does not contribute in the far field.

The resolved stress σ is defined by its relation with the Peach-Koehler force $F_k = b\sigma t_k$, with \mathbf{t} the slip direction, which for a gliding edge is the direction of the Burgers vector. The Peach-Koehler force is $F_k = \epsilon_{kjm} \tau_m b_i \sigma_{ij}$ so we conclude that, for gliding edge

$$\sigma = \epsilon_{kjm} \sigma_{ij} \tau_m t_i t_k. \quad (\text{E3})$$

Choosing a fixed direction for $\tau = \mathbf{e}_3$ and $\mathbf{t} = \mathbf{e}_1$ leads to $\sigma = \sigma_{12}$. Note that this simplification is the price to pay to have a scalar equation on the stress tensor. In our case where τ and \mathbf{t} vary for randomly oriented segments, this would not be possible. We can now calculate the stress using $\sigma = c_{12nm} \beta_{nm}$ in Eq. (E1). We get

$$\begin{aligned} \sigma(\mathbf{x}, t) = & \int \int_{\mathcal{L}} dt' ds \rho b c_{12nm} \epsilon_{nlh} t_i \tau_h t_l \\ & \times \frac{\partial}{\partial t} G_{im}^0(\mathbf{x} - \mathbf{X}, t - t') \dot{X}_l(s, t') \\ = & - \int \int_{\mathcal{L}} dt' ds \rho \mu b \frac{\partial}{\partial t} G_{11}^0(\mathbf{x} - \mathbf{X}, t - t') \dot{X}_1(s, t'), \end{aligned} \quad (\text{E4})$$

where it has been used that τ keeps the same direction at

leading order. The Green function G_{11}^0 , denoted G^0 hereafter, satisfies the wave equation

$$\rho \frac{\partial^2}{\partial t^2} G^0(\mathbf{x}, t) - \mu \frac{\partial^2}{\partial x_2^2} G^0(\mathbf{x}, t) = \delta(t) \delta(\mathbf{x}), \quad (\text{E5})$$

for a one dimensional wave (propagating along x_2). We now use $\mathbf{X} \approx \mathbf{X}_0$ in the Green function and integrating by part (using $\partial G / \partial t = -\partial G / \partial t'$), we get, in a modified form

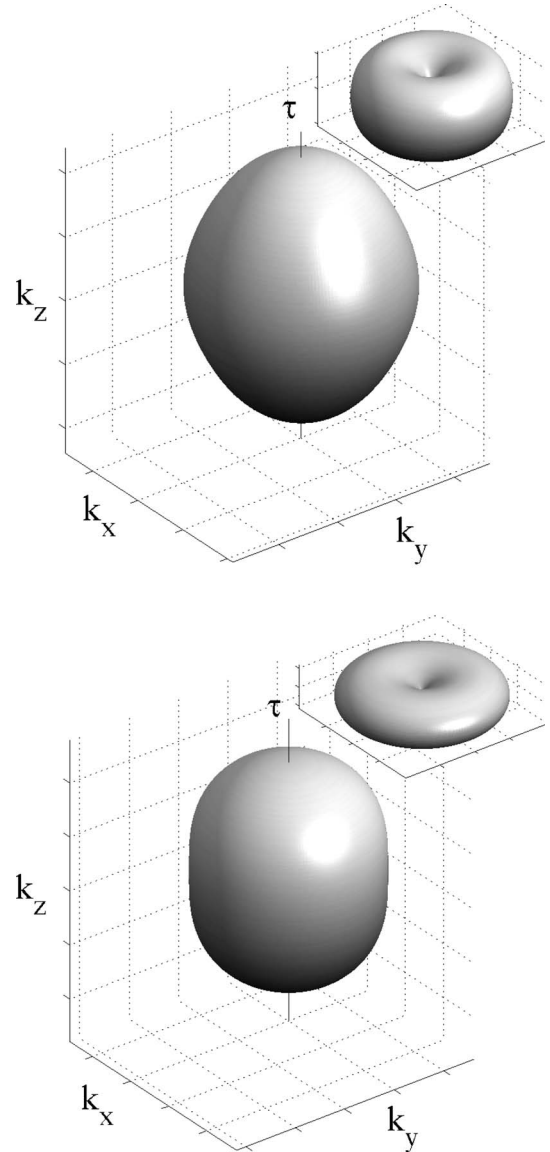


FIG. 5. Modified wave numbers (a) K_T and (b) K_L as a function of the incident wave direction, in a medium containing dislocation segments randomly located in space but all pointing along the \mathbf{e}_3 direction, and Burgers vector randomly oriented in the $(\mathbf{e}_1, \mathbf{e}_2)$ -plane. The deviation from a spherical shape indicates the anisotropy of the medium. Insets show the change in wave vectors $(K_a - k_a)/k_a$, $a = L, T$.

$$\begin{aligned} \sigma(\mathbf{x}, t) = & -\rho \int dt' dx' G^0(\mathbf{x} - \mathbf{x}', t - t') \\ & \times \int_{\mathcal{L}} ds \mu b \ddot{X}(s, t') \delta(\mathbf{x}' - \mathbf{X}_0). \end{aligned} \quad (\text{E6})$$

It is now sufficient to see that σ is a convolution between the Green function and a source term to deduce the modified wave equation for σ in the presence of a moving dislocation

$$\rho \frac{\partial^2}{\partial t^2} \sigma(\mathbf{x}, t) - \mu \frac{\partial^2}{\partial x_2^2} \sigma(\mathbf{x}, t) = -\mu b \int_{\mathcal{L}} ds \ddot{X}(s, t) \delta(\mathbf{x} - \mathbf{X}_0). \quad (\text{E7})$$

This equation corresponds to Eq. (3.4), whose average over all realizations of ensembles of dislocations randomly

located, but not randomly oriented, gives the modified wave equation used by Granato and Lücke in their model.

APPENDIX F: DISPERSION RELATION IN A CONFIGURATION CLOSE TO THE GL CONFIGURATION

The scalar model of Granato and Lücke concerns a particular configuration where all dislocations are parallel with the same Burgers vectors. A configuration that is intermediate between GL and ours is obtained by allowing, in the GL configuration, the Burgers vectors to take any orientation in the $(\mathbf{e}_1, \mathbf{e}_2)$ -plane, perpendicular to $\boldsymbol{\tau}$. In this case the calculation of the mass operator must be performed averaging $\mathbf{M} \hat{\mathbf{k}}' \mathbf{k} \mathbf{M}$ in Eq. (C2) over the angle θ_n in $\mathbf{M} = \mathbf{n}' \mathbf{t} + t' \mathbf{n}$ [with $\mathbf{n} = (\cos \theta_n; \sin \theta_n)$ and $\mathbf{t} = (-\sin \theta_n; \cos \theta_n)$].

We get from Eqs. (C2),

$$\begin{aligned} \Sigma(\mathbf{k}) = & -\frac{8}{\pi^2} \frac{(\mu b)^2 S(\omega)}{m \omega^2} nL \int d\theta_n \cos^2 2\theta_n \begin{pmatrix} (k_2 - \tan 2\theta_n k_1)^2 & (k_2 - \tan 2\theta_n k_1)(k_1 + \tan 2\theta_n k_2) & 0 \\ (k_2 - \tan 2\theta_n k_1)(k_1 + \tan 2\theta_n k_2) & (k_1 + \tan 2\theta_n k_2)^2 & 0 \\ 0 & 0 & 0 \end{pmatrix} \\ = & -\frac{1}{2} \rho c_T^2 s_1 (k_1^2 + k_2^2) \begin{pmatrix} 1 & 0 & 0 \\ 0 & 1 & 0 \\ 0 & 0 & 0 \end{pmatrix} \end{aligned} \quad (\text{F1})$$

with

$$s_1 = \frac{8}{\pi^2} \frac{\rho b^2 S(\omega)}{m \omega^2} nL c_T^2,$$

so that the effective wave numbers are given by the poles of $\langle G \rangle^{-1}(\mathbf{k})$

$$\langle G \rangle^{-1}(\mathbf{k}) = G^{0-1}(\mathbf{k}) - \Sigma(\mathbf{k}), \quad (\text{F2})$$

with G^0 given in Eq. (B3). Using $\hat{\mathbf{k}} = [\cos \varphi \cos \theta; \cos \varphi \sin \theta; \sin \varphi]$, it is straightforward to find the discriminant of $\langle G \rangle^{-1}$,

$$\begin{aligned} \Delta_{\langle G \rangle} = & -\rho c_T^2 (k^2 - k_T^2) \{ (k^2 - k_T^2) (\gamma^2 k^2 - k_T^2) + s_1 k^2 \cos^2 \varphi [k^2 \\ & - k_T^2 + (\gamma^2 - 1) k^2 g(\varphi)] \}, \end{aligned} \quad (\text{F3})$$

with $g(\varphi) = (1 + \sin^2 \varphi)/2$. The modified wave numbers being

close to the wave numbers k_L, k_T , we get at leading order in s_1 ,

$$K_T = k_T \left(1 - \frac{s_1}{4} \cos^2 \varphi (1 + \sin^2 \varphi) \right),$$

$$K_L = k_L \left(1 - \frac{s_1}{4} \cos^4 \varphi \right). \quad (\text{F4})$$

The modified wave numbers are shown in Fig. 5, the deviation from a spherical shape illustrates the anisotropy of this medium. Of course, here, the anisotropy only concerns the $\boldsymbol{\tau}$ direction.

¹A. Hikata, R. Truel, A. Granato, B. Chick, and K. Lücke, J. Appl. Phys. **27**, 386 (1956).

²H. M. Ledbetter, J. Phys. D **13**, 1879 (1980).

³H. M. Ledbetter and C. Fortunko, J. Mater. Res. **10**, 1352 (1995).

⁴H. Ogi, M. Hirao, and T. Honda, J. Acoust. Soc. Am. **98**, 458

(1995).

⁵H. Ogi, M. Hirao, and K. Minoura, J. Appl. Phys. **81**, 3677 (1997).

⁶H. Ogi, N. Suzuki, and M. Hirao, Metall. Mater. Trans. A **29A**, 2987 (1998).

- ⁷W. Johnson, *J. Appl. Phys.* **83**, 2462 (1998).
- ⁸H. Ogi, H. M. Ledbetter, S. Kim, and M. Hirao, *J. Acoust. Soc. Am.* **106**, 660 (1999).
- ⁹H. Ogi, A. Tsujimoto, M. Hirao, and H. Ledbetter, *Acta Mater.* **47**, 3745 (1999).
- ¹⁰M. Hirao, H. Ogi, N. Suzuki, and T. Ohtani, *Acta Mater.* **48**, 517 (2000).
- ¹¹H. Ogi, N. Nakamura, M. Hirao, and H. Ledbetter, *Ultrasonics* **42**, 183 (2004).
- ¹²T. Ohtani, H. Ogi, and M. Hirao, *Int. J. Solids Struct.* **42**, 2911 (2005).
- ¹³M. W. Barsoum, M. Radovic, T. Zhen, P. Finkel, and S. R. Kalidindi, *Phys. Rev. Lett.* **94** 085501 (2005).
- ¹⁴A. V. Granato and K. Lücke, in *Physical Acoustics*, edited by W. P. Mason (Academic, New York, 1966), Vol. 4A.
- ¹⁵A. V. Granato and K. Lücke, *J. Appl. Phys.* **27**, 583 (1956).
- ¹⁶A. V. Granato and K. Lücke, *J. Appl. Phys.* **27**, 789 (1956).
- ¹⁷R. M. Stern and A. V. Granato, *Acta Metall.* **10** 358 (1962).
- ¹⁸K. Lücke and A. V. Granato, *Phys. Rev. B* **24**, 6991 (1981).
- ¹⁹G. A. Kneezel and A. V. Granato, *Phys. Rev. B* **25**, 2851 (1982).
- ²⁰A. Maurel, J.-F. Mercier, and F. Lund, *Phys. Rev. B* **70**, 024303 (2004).
- ²¹A. Maurel, V. Pagneux, D. Boyer, and F. Lund, *Mater. Sci. Eng., A* **400-401**, 222 (2005).
- ²²A. Maurel, V. Pagneux, D. Boyer, and F. Lund (unpublished).
- ²³A. Maurel, J.-F. Mercier, and F. Lund, *J. Acoust. Soc. Am.* **115**, 2773 (2004).
- ²⁴A. Maurel, V. Pagneux, F. Barra, and F. Lund, preceding paper, *Phys. Rev. B* **72**, 174110 (2005) (called Paper I in the text).
- ²⁵L. L. Foldy, *Phys. Rev.* **67**, 107 (1945).
- ²⁶M. Lax, *Rev. Mod. Phys.* **23**, 287 (1951).
- ²⁷M. Lax, *Phys. Rev.* **85**, 621 (1952).
- ²⁸A. Ishimaru, *Wave Propagation and Scattering in Random Media* (IEEE/OUP, New York, 1997).
- ²⁹P. Sheng, *Scattering and Localization of Classical Waves in Random Media* (World Scientific, Singapore, 1990).
- ³⁰P. Sheng, *Introduction to Wave Scattering, Localization, and Mesoscopic Phenomena* (Academic, New York, 1995).
- ³¹B. Velicky, <http://parthe.lpthe.jussieu.fr/DEA/velicky.html>
- ³²E. Zolotoyabko, D. Shilo, and E. Lakin, *Mater. Sci. Eng., A* **309-310**, 23 (2001).
- ³³D. Shilo and E. Zolotoyabko, *Ultrasonics* **40**, 921 (2002).
- ³⁴D. Shilo and E. Zolotoyabko, *Phys. Rev. Lett.* **91**, 115506 (2003).
- ³⁵M. Peach and J. S. Koehler, *Phys. Rev.* **80**, 436 (1950).
- ³⁶J. S. Koehler, in *Imperfections in Nearly Perfect Crystals*, edited by W. Shockley *et al.* (Wiley, New York, 1952).
- ³⁷F. Lund, *J. Mater. Res.* **3**, 280 (1988).
- ³⁸M. Hiratani and E. M. Nadgorny, *Acta Mater.* **49**, 4337 (2001).
- ³⁹E. M. Nadgorny, *Prog. Mater. Sci.* **31**, 1 (1988).
- ⁴⁰T. Mura, *Philos. Mag.* **8**, 843 (1963).
- ⁴¹J. Wang, Q. F. Fang, and Z. G. Zhu, *Phys. Status Solidi A* **169**, 43 (1998).
- ⁴²S. Kenderian, T. P. Berndt, R. E. Green, Jr., and B. B. Djordjevic, *Mater. Sci. Eng., A* **348**, 90 (2003).
- ⁴³S. Kenderian, T. P. Berndt, R. E. Green, Jr., and B. B. Djordjevic, *J. Test. Eval.* **31**, 98 (2003).
- ⁴⁴T. Suzuki, M. Aoki, and A. Ikushima, *Acta Metall.* **12**, 1231 (1964).
- ⁴⁵W. P. Mason and A. Rosenberg, *Phys. Rev.* **151** 434 (1966).
- ⁴⁶T. Ninomiya, *J. Phys. Soc. Jpn.* **36**, 399 (1974).
- ⁴⁷B. Zadler, J. H. L. Le Rousseau, J. A. Scales, and M. L. Smith, *Geophys. J. Int.* **156**, 154 (2004); A. Migliori, and J. L. Sarao, *Resonant Ultrasound Spectroscopy* (Academic, New York, 1997).
- ⁴⁸S. S. Andrews, *J. Chem. Educ.* **81**, 877 (2004).